



INDONESIAN JOURNAL ON GEOSCIENCE

Geological Agency
Ministry of Energy and Mineral Resources

Journal homepage: <http://ijog.geologi.esdm.go.id>
ISSN 2355-9314, e-ISSN 2355-9306



Tectonic Model of Bali Island Inferred from GPS Data

CECEP SULAEMAN, SRI HIDAYATI, AMALFI OMANG, and IMAM CATUR PRIAMBODO

Centre for Volcanology and Geological Hazard Mitigation, Geological Agency
Jln. Diponegoro No. 57 Bandung, West Java, Indonesia

Corresponding author: cecepsula@gmail.com

Manuscript received: March 9, 2017; revised: June 21, 2017;
approved: January 15, 2018; available online: March 8, 2018

Abstract - Seven periods of GPS campaign have been conducted for three years since March 2013 - October 2015 on fourteen GPS sites across Bali Island. The GAMIT/GLOBK 10.6 version was used to compute data with respect for thirteen reference sites of International Terrestrial Reference Frame (ITRF) 2008 surrounding Bali. The result shows that horizontal displacement varies between 1.93 and 22.53 mm/yr dominantly northeastward. Vertical displacement ranges at -184.34 to 33.79 mm/yr. The result of modeling using Coulomb 3.3 version indicates the deformation in Bali was mostly contributed by subduction at the southern part, West and East Flores Back-Arc Thrust at the north, Lombok Strait Fault and a fault at the eastern coast of Bali with the estimation maximum magnitude of 7.1, 6.6, 6.8, 5.8, and 5.2, respectively.

Keywords: Bali, deformation, GPS campaign, horizontal displacement, subduction

© IJOG - 2018. All right reserved

How to cite this article:

Sulaeman, C., Hidayati, S., Omang, A., and Priambodo, I.C., 2018. Tectonic Model of Bali Island Inferred from GPS Data. *Indonesian Journal on Geoscience*, 5 (1), p.81-91. DOI: [10.17014/ijog.5.1.81-91](https://doi.org/10.17014/ijog.5.1.81-91)

INTRODUCTION

Since 1818, Bali Island has experienced sixteen destructive earthquakes (Supartoyo *et al.*, 2014). A strong earthquake occurred in 1818 with the intensity of VII MMI causing 1500 people lost their lives. Another destructive earthquake with magnitude of 6.1 struck Seririt in 1976 killing over than 559 people. The most recent destructive one occurred on October 13, 2011 creating some damages (Sulaeman, 2011).

Tectonically, Bali Island and Nusa Tenggara are part of Lesser Sunda Islands, which are defined as a group of small islands situated between east of Java and Banda Islands (Figure 1). The tectonic of this region is dominated by the col-

lision between Australia and Eurasia Plates, as an earthquake source in the south of Bali. The Australia Plate subducting beneath Eurasia Plate was at a rate of 67 ± 7 mm/yr in $N11^\circ E \pm 4^\circ$ direction (Tregoning *et al.*, 1994). Bock *et al.* (2003) revealed that Sunda Shelf block is estimated to be moving 6 ± 3 mm/yr SE relative to Eurasia. Another earthquake source which affected Bali originates from Flores Back-Arc Thrust extending from the north of Bali on the west and East Nusa Tenggara on the east side. Flores Back-Arc thrusting has been recognized by Hamilton (1979) to be behind Alor and Pantar Islands in the east and from central Flores to central Sumbawa in the west. Silver *et al.* (1983) suggested that the Flores thrust zone disappears beneath Bali

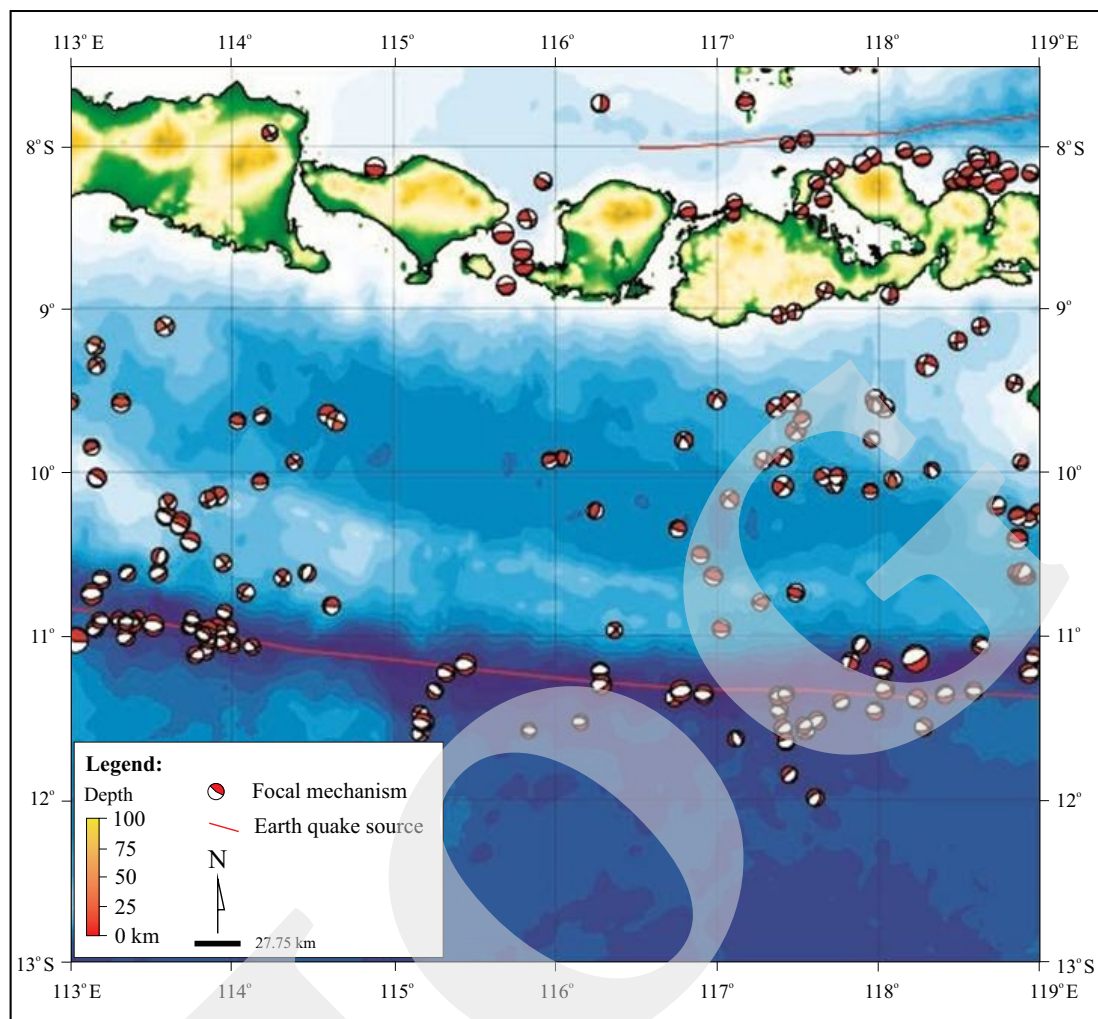


Figure 1. Seismicity of Bali during 1976 - 2015 at depth 0 - 60 km (Source Data CMT Catalog).

Basin. In contrast, Koulali *et al.* (2016) reveals Flores Back-Arc continues westward until Kendeng Thrust. A seismotectonic study (Soehaimi, 2015) found a fault scarp at N 50° E direction at Lombok Strait, eastern Bali, parallel to the eastern coastal zone.

Earthquake source characteristics are important in order to define an earthquake hazard level in a certain area (Figure 1). Source characteristic information (location, geometry, slip rate, and maximum magnitude) can be obtained from geological and geodetic methods. In this study, a geodetic method using GPS measurement was used to identify the characteristic of the earthquake source. The survey had been conducted for three years since 2013 to 2015. This paper presents its result and discusses the displacement pattern as

well as performs a model describing earthquake sources affect Bali and surrounding areas.

GPS Survey And Analysis

GPS survey is a method which is often used to analyze deformation associated with crustal fault activities by observing the displacement pattern. A GPS survey can be carried out either with episodic or continuous measurements. In contrast to a continuous observation approach, an episodic method, also known as a campaign survey, is conducted by careful observing changes with a specified interval, for instance, once or twice a year. A deformation rate requires a high precision level which is generally at the level of mm/year.

GPS surveys in Bali were conducted seven times from 2013 to 2015: in March 2013, June

2013, September 2013, April 2014, October 2014, April 2015, and October 2015 using Trimble R7, R8, and NetRS. The measurement of each site takes two DOYs (Day of Year) and at least 8 hours/day of duration. There are fourteen GPS sites across Bali as seen in Figure 2: BMKG (BMKG Kuta), KLKG (Kelungkung Dam), SKWT (SMAN Sukowati), TGLG (Polsek Tegallalang), SSUT (Polsek Susut), BTUR (Batur Observatory), KTMN (SMPN Kintamani), SKDN (Sukadana Village), BNJR (SMPN Banjar), PMTR (Pemuteran Village), CEGI (Cegi Village), JMBR (Jembrana City), KASM (BMKG Karangasem), and NSDA (SMAN Nusa Dua). CEGI is a continuous GPS site.

Raw data in RINEX format were processed using GAMIT-GLOBK software 10.6 version (Herring *et al.*, 2015) in combination with global network of thirteen International GNSS Service (IGS) tracking sites as reference frames. Those IGS (<http://igsceb.jpl.nasa.gov/>) sites are BAKO (Cibinong), COCO (Cocos), DARW (Darwin), GUAM (Guam), NTUS (Nanyang), PIMO (Ma-

nila), DGAR (Deigo Garsia), HYDE (Hyderabad), IISC (Bangalore), KARR (Karratha), KUNM (Kunming), LAE (Lae), and MALD (Maldives). Due to a technical reason, the KASM, NSDA, SKWT, and BMKG sites were only surveyed three times. The available data of CEGI started on January - September 2013 and February 2014.

For each day measurement, the dual-frequency carrier phase and pseudo-range observations from all sites were taken into account in processing the data. The International Terrestrial Reference Frame (ITRF) 2008 was used as a reference system. The ITRF 2008 is the realization of International Terrestrial Reference System (ITRS) where its centre is located on geocentric (the centre of mass of earth) with axes oriented consistently towards BIH (the Bureau International de l'Heure) at epoch 1984.0, and its length is defined in meters (Kuncoro, 2013).

To find out the displacement at each GPS site, the coordinate in the geocentric system was converted to topocentric with respect for an epoch on a specific reference. In this case, the first

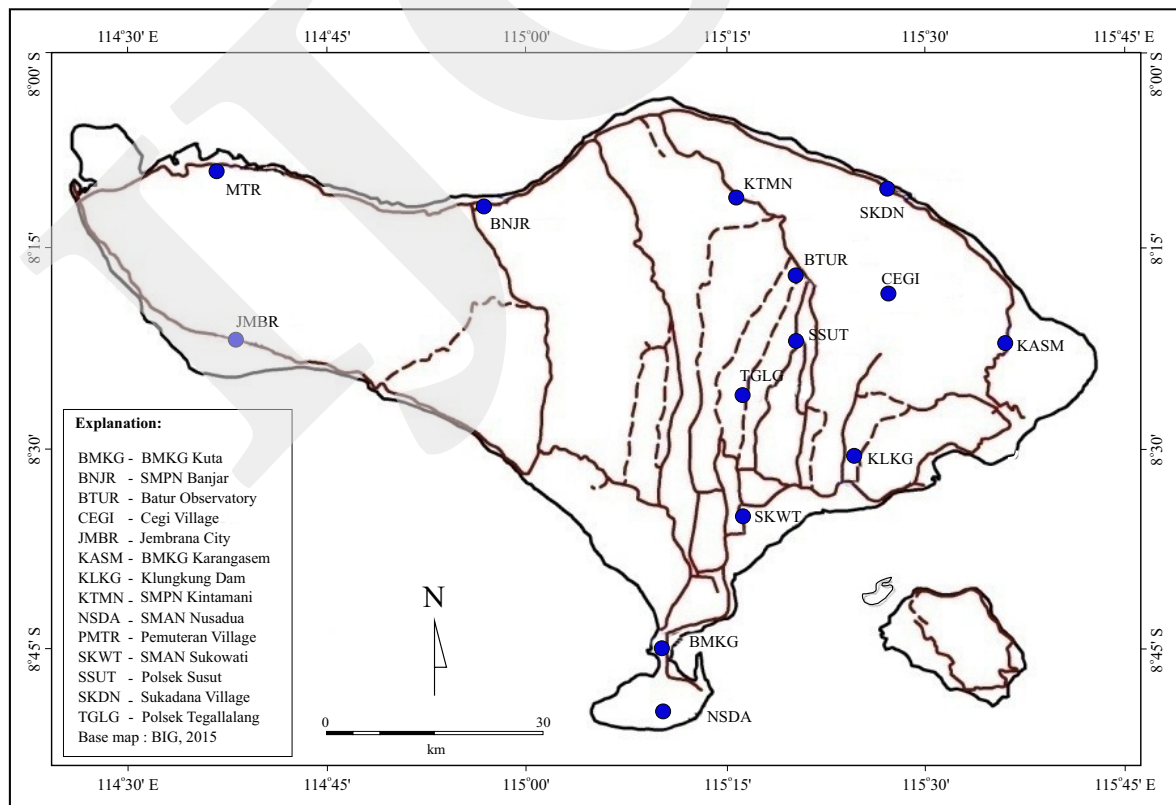


Figure 2. Map of GPS sites (solid circles) in Bali Island.

measurement coordinate at each GPS site was used as a starting point. The velocity vector can be estimated from the change of the topocentric coordinate system. To eliminate the global influence, horizontal velocity component was corrected by the movement of Sunda Block using Plate-Motion-Calculator in Morvel 2010 model which was obtained from the website <https://www.unavco.org>. Sunda Block Euler rotation parameters which were used in this calculation was Euler polars coordinate of 46.202°N and -85.899°E and the angular velocity of 0.370° /million years (Kuncoro, 2013). Furthermore, in order to find the best fit model of the earthquake source to the available velocity data, the Coulomb 3.3 software (Toda *et al.*, 2011) was performed.

RESULTS AND ANALYSIS

Data obtained from the GPS processing are displacement of position which was visualized in a time series. It describes the movement of a GPS site within a specific time interval. From the time series of position changes, the velocity vector value of each GPS movement site can be estimated using the least square method. For example, displacement (north, east, and up) for SSUT site during the period of March 2013 - October 2015 is shown in Figure 3. The obtained displacement are -1.39 mm/yr , 28.25 mm/yr , and 1.41 mm/yr for component of north, east, and up, respectively.

The velocity for each GPS site is shown in Table 1 and Figure 4. Normalized root mean square (nrms) was estimated from differences between the observations and calculated phase and the value of the weighted root mean square residual (wrms) representing short-term correlation within data, as shown in Figure 4 and Table 1. The horizontal displacement of Bali tends to east-southeast (Figure 4) before being corrected by Sunda Block, except NSDA site.

According to Table 1 and Figure 4 the velocity values vary 22.09 mm/yr to 33 mm/yr with the error bar ranging from 0.99 mm/yr to 20.08 mm/yr for north component, and 1.26 mm/yr to

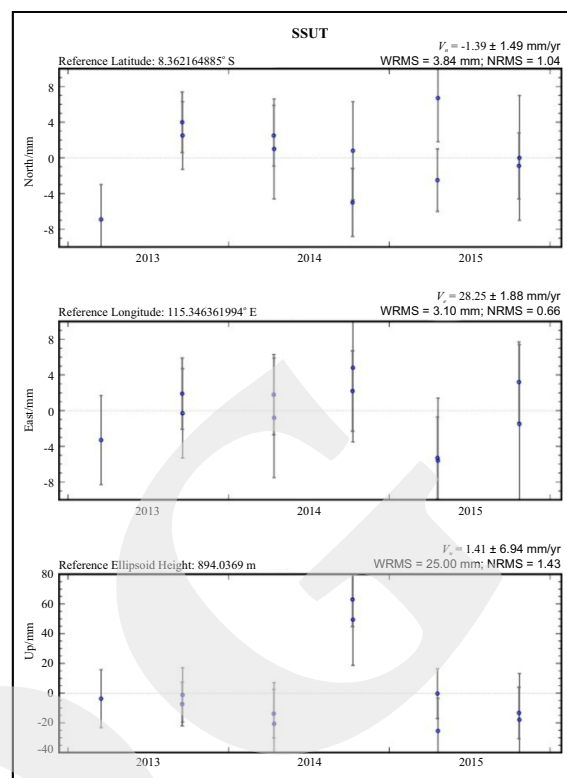


Figure 3. Time series position of the survey period for SSUT site.

23.72 mm/yr for the east one. The lowest velocity was recorded at BTUR (22.09 mm/yr) and the highest at KLKG (49.29 mm/yr). Meanwhile, the vertical velocity varies between -184.34 mm/yr (downward) to 33.79 mm/yr (upward). The lowest downward was recorded at KLKG (-184 mm/yr), and the highest upward at PMTR (39 mm/yr). The error bar for horizontal measurement relatively seems to be better compared to the vertical one. The large error bar recorded at KLKG for both vertical and horizontal could be due to vibration noise from the stream since the site is located just on the river bank.

The Sunda Block moves 27 mm/yr in SE direction as seen in Figure 5. Figure 6 and Table 2 show horizontal velocity for each GPS site after being corrected by the Sunda Block movement. The velocity value varies at 1.93 mm/yr to 22.53 mm/yr , and tends to NE direction, except for NSDA, BTUR, and KASM northward and KLKG eastward. The smallest value was recorded at PMTR (1.93 mm/yr) and the largest at KLKG (22.53 mm/yr).

Table 1. Velocity of Each GPS Site During the Period of April 2013 - October 2015

Site	North	Component Velocity (mm/year)			Vertical	$\pm V$	Resultant Horizontal
		$\pm N$	East	$\pm E$			
BMKG	-9.28	2.52	28.95	2.31	-67.32	16.01	30.40
BNJR	-7.47	1.43	31.86	1.93	1.37	7.57	32.72
BTUR	-1.26	0.99	22.05	1.26	-3.34	13.13	22.09
CEGI	-8.67	4.67	27.04	4.47	5.25	12.96	28.40
JMBR	-6.48	5.39	32.74	7.98	33.73	25.7	33.38
KASM	-5.04	12.01	24.28	14.91	-33.04	73.54	24.80
KLKG	-11.32	20.08	47.97	23.72	-184.34	90.44	49.29
KTMN	-4.70	2.38	28.94	3.01	-12.71	11.01	29.32
NSDA	6.15	4.70	25.21	5.15	-50.07	33.25	25.95
PMTR	-9.06	2.36	27.33	3.04	39.77	10.28	28.79
SKDN	0.14	1.22	28.07	1.91	-1.61	6.74	28.07
SKWT	-2.52	9.45	37.02	11.42	-70.42	45.68	37.11
SSUT	-1.39	1.49	28.25	1.88	1.41	6.94	28.28
TGLG	-3.68	1.96	29.34	2.66	-60.18	9.41	29.57

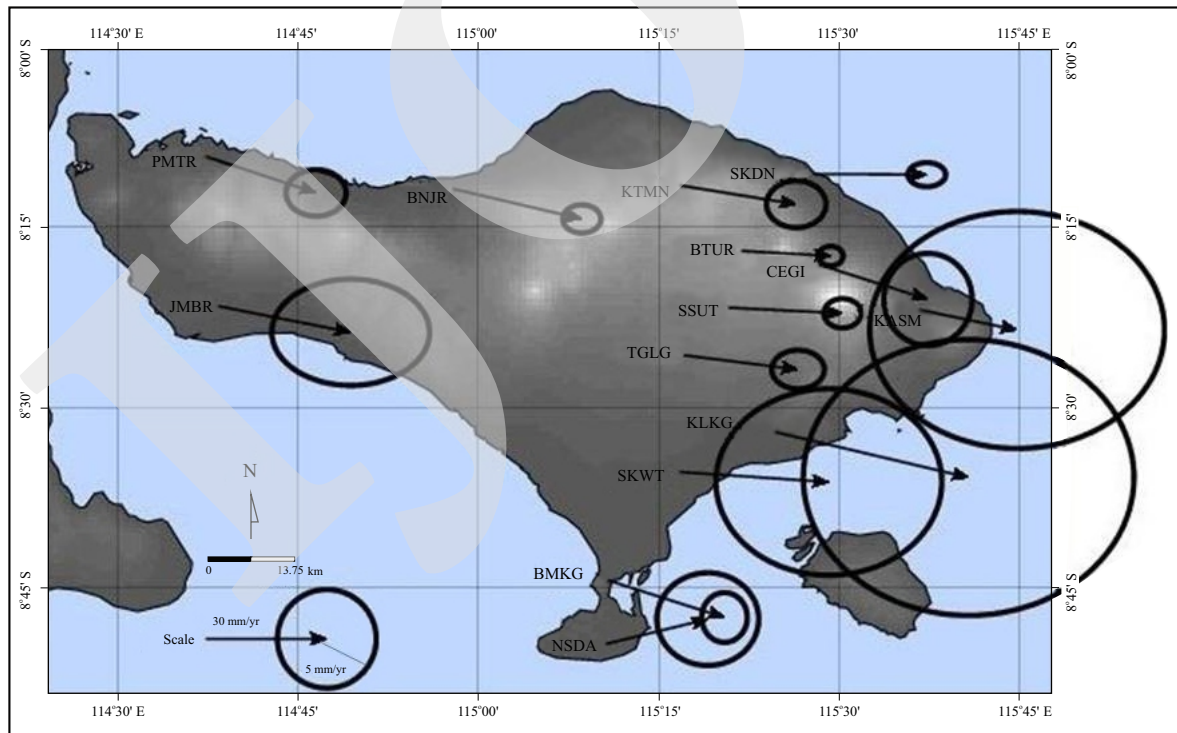


Figure 4. Velocity for each Bali GPS site and their error bar during April 2013 - October 2015 (ITRF 2008).

In order to find out the cause of surface deformation in Bali, a model of earthquake sources was applied and computed using Coulomb Version 3.3 (Toda *et al.*, 2011). For modeling, only horizontal

velocities were used, and any vertical rate was not included since they have large uncertainties. Five earthquake source parameters were defined as an input, namely subduction at the southern part

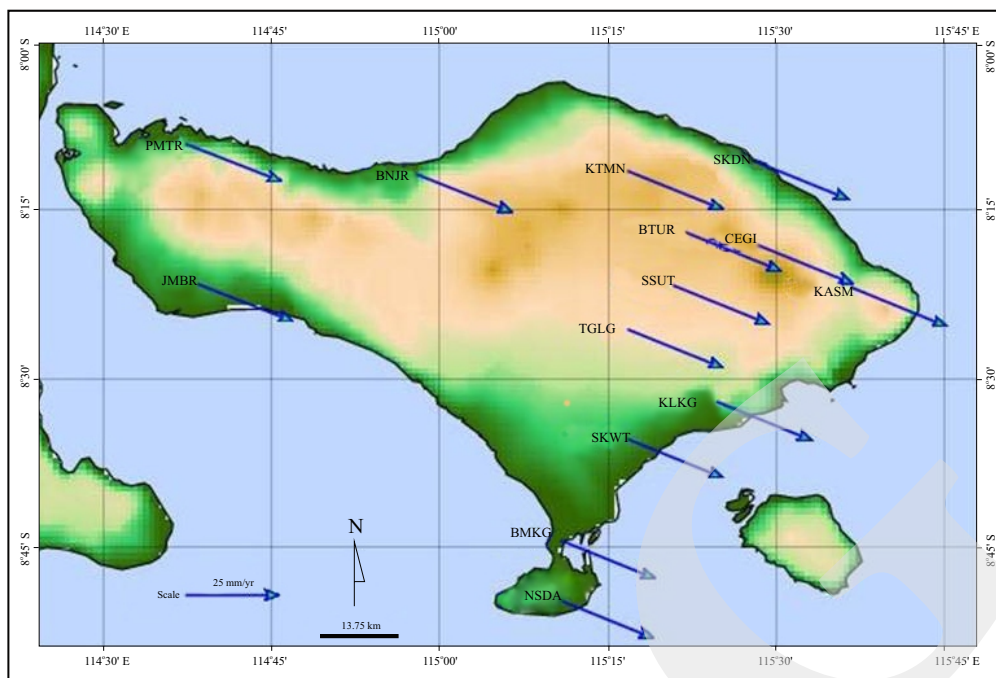


Figure 5. Velocity model for Sunda Block at Bali GPS sites.

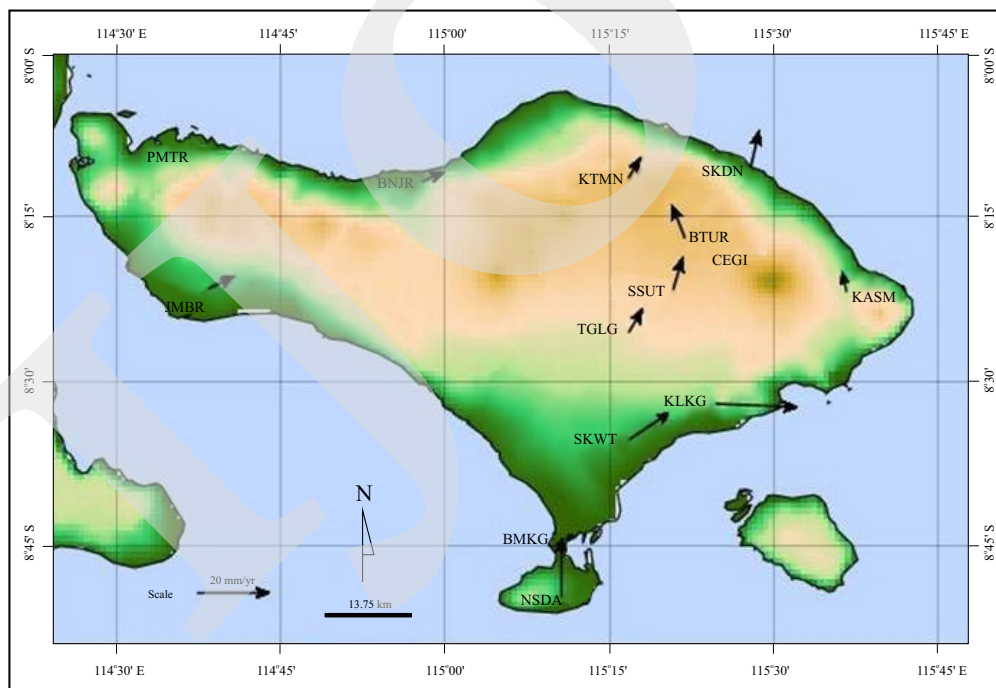


Figure 6. Velocity for each GPS site with respect for Sunda Block.

of Bali with length 427.27 km including Sumba Megathrust, West Flores Back-Arc Thrust (170.50 km), and East Flores Back-Arc Thrust (277.13 km) in the north, Lombok Strait Fault (54.75 km), and a fault 15.86 km in length on the eastern coast of Bali (Figure 7, Table 3). Those sources

are considered to affect most deformation across Bali. The result of modeling using the best fit approach between the observed and calculated data can be seen in Table 4. The five source models produce GPS velocity at 0.81 mm/yr to 13.51 mm/yr northeastward (Figure 8). This direction is in

Table 2. Component of Horizontal Velocity for Each GPS Site during April 2013 - October 2015 with respect for Sunda Block

Site	East (mm/yr)	North (mm/yr)	Resultant Horizontal (mm/yr)
BMKG	3.61	0.97	3.74
BNJR	6.23	2.68	6.79
BTUR	-3.54	9.08	9.74
CEGI	1.46	1.72	2.25
JMBR	7.21	3.52	8.02
KASM	-1.27	5.41	5.56
KLKG	22.51	-0.96	22.53
KTMN	3.30	5.60	6.50
NSDA	-0.08	16.40	16.40
PMTR	1.69	0.93	1.93
SKDN	2.42	10.24	10.53
SKWT	11.59	7.78	13.96
SSUT	2.70	8.94	9.34
TGLG	3.83	6.62	7.65

accordance with sites of KTMN, SKWT, CEGI, and TGLG. Table 4 shows the difference between observation and calculation of each GPS site. The site of KLKG has the largest difference between

-20.52 mm/yr and 6.33 mm/yr for east and north components, respectively. Other sites show 0.19 mm/yr to 9.65 mm/yr for the east component, and 0.52 mm/yr to -16.52 mm/yr for the north one.

DISCUSSION

Figure 1 shows earthquake sources around Bali. In Bali and Nusa Tenggara, most of the deformation of the island arc can be attributed to collision with the Australian Continent. At the southern part, the earthquakes are dominated by reverse mechanism. This shows that the earthquakes are associated with the subduction zone, such as destructive earthquakes in Buleleng (1862) and the most recent in Nusa Dua (2011) (Figure 9a, b). Earthquakes at the northern part of Bali and Nusa Tenggara are also dominated by thrusting mechanism (Figure 1). According to McCaffrey and Nabelek (1987) the causes of thrust fault are due to lower crustal depths and shallowly southward dipping nodal planes beneath the Bali Basin. No obvious earthquakes

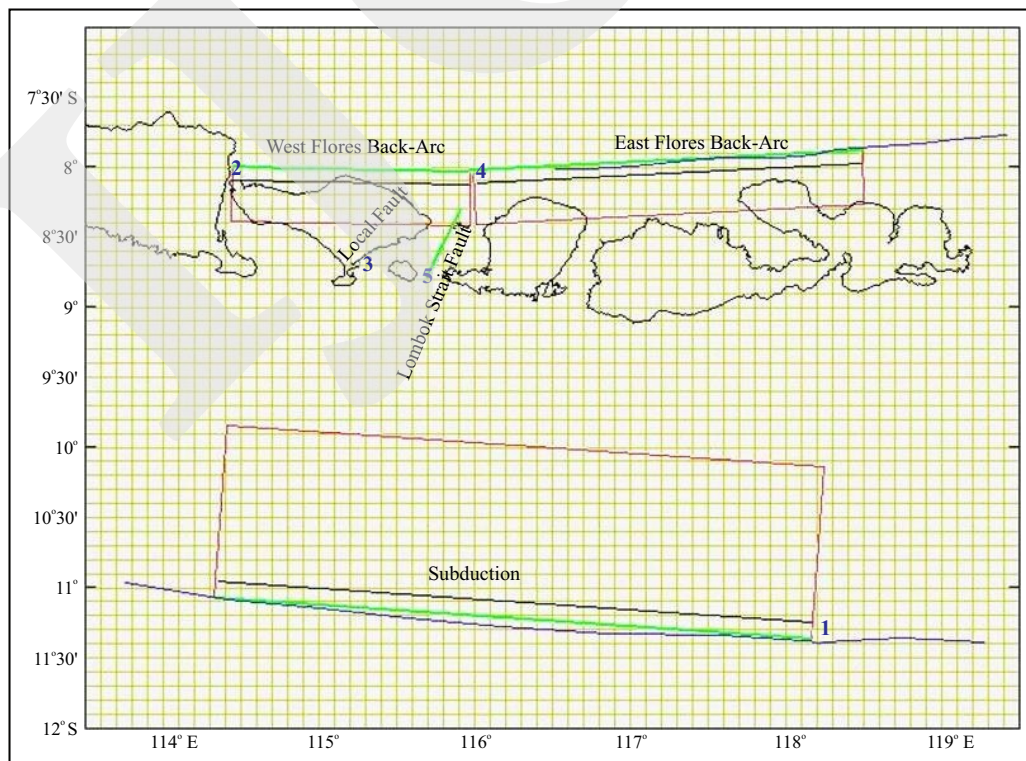


Figure 7. Earthquake source model.

Table 3. Input Parameter of Earthquake Source Model

Earthquake source	Length (km)	Width (km)	Strike (°)	Top Depth (km)	Bottom Depth (km)	Dip (°)	Reverse Slip (m)	Right-lateral Slip (m)	Moment magnitude (Mw)
Subduction (Sumba Megathrust)	427.27	133.47	273.93	0	50	22	0.03	0.00	7.1
West Flores Back Arc	170.50	44.05	90.93	0	20	27	0.03	-0.009	6.6
East Flores Back Arc	277.13	31.11	87.08	0	20	27	0.04	-0.005	6.8
Lombok Strait Fault	54.75	15.00	26.91	0	15	90	0	-0.02	5.8
Local Fault	15.04	10	57.40	0	10	90	0.002	0.015	5.2

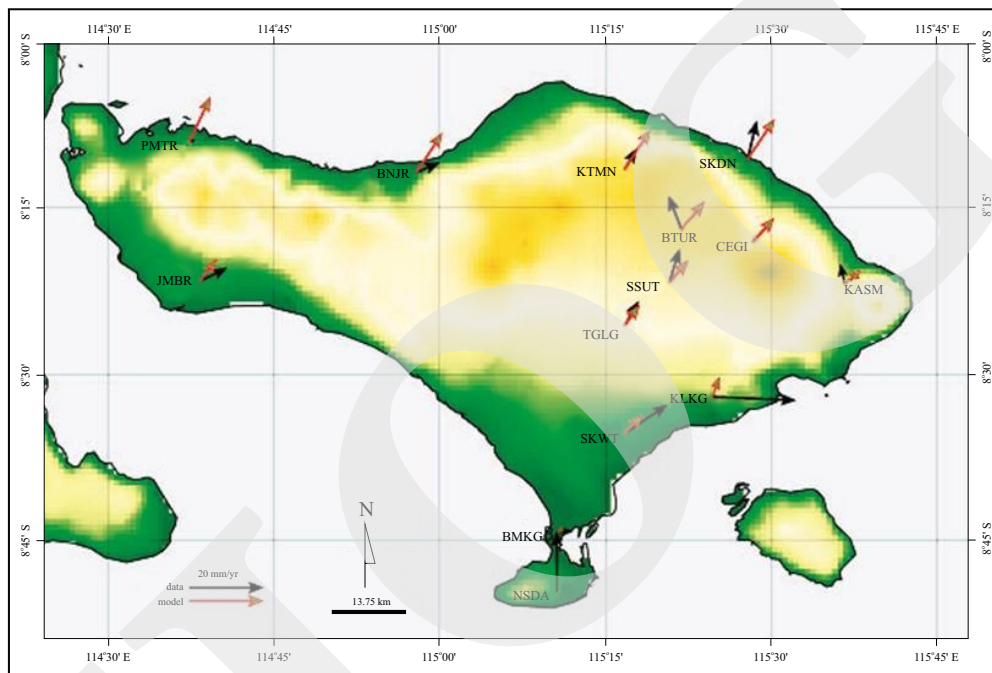


Figure 8. Horizontal velocity vectors in Bali. The red and black colours represent calculated and observed data, respectively.

Table 4. Observed and Calculated Velocity for Each Bali GPS Site

Site	Observed (mm)		Calculated (mm)		Calculated - Observed (mm)	
	East (E)	North (N)	East (E)	North (N)	East (Ec-o)	North (Nc-o)
BMKG	3.61	0.97	1.12	1.64	-2.49	0.67
BNJR	6.23	2.68	6.94	10.66	0.71	7.98
BTUR	-3.54	9.08	6.11	7.53	9.65	-1.55
CEGI	1.46	1.72	5.85	6.54	4.40	4.82
JMBR	7.21	3.52	4.41	5.99	-2.80	2.47
KASM	-1.27	5.41	4.50	3.84	5.77	-1.57
KLKG	22.51	-0.96	1.99	5.37	-20.52	6.33
KTMN	3.30	5.60	7.05	10.66	3.75	5.06
NSDA	-0.08	16.40	0.77	0.26	0.86	-16.15
PMTR	1.69	0.93	5.75	12.23	4.06	11.30
SKDN	2.42	10.24	7.28	10.76	4.86	0.52
SKWT	11.60	7.78	5.06	5.00	-6.54	-2.78
SSUT	2.70	8.94	4.98	5.80	2.27	-3.14
TGLG	3.83	6.62	4.02	5.51	0.19	-1.11

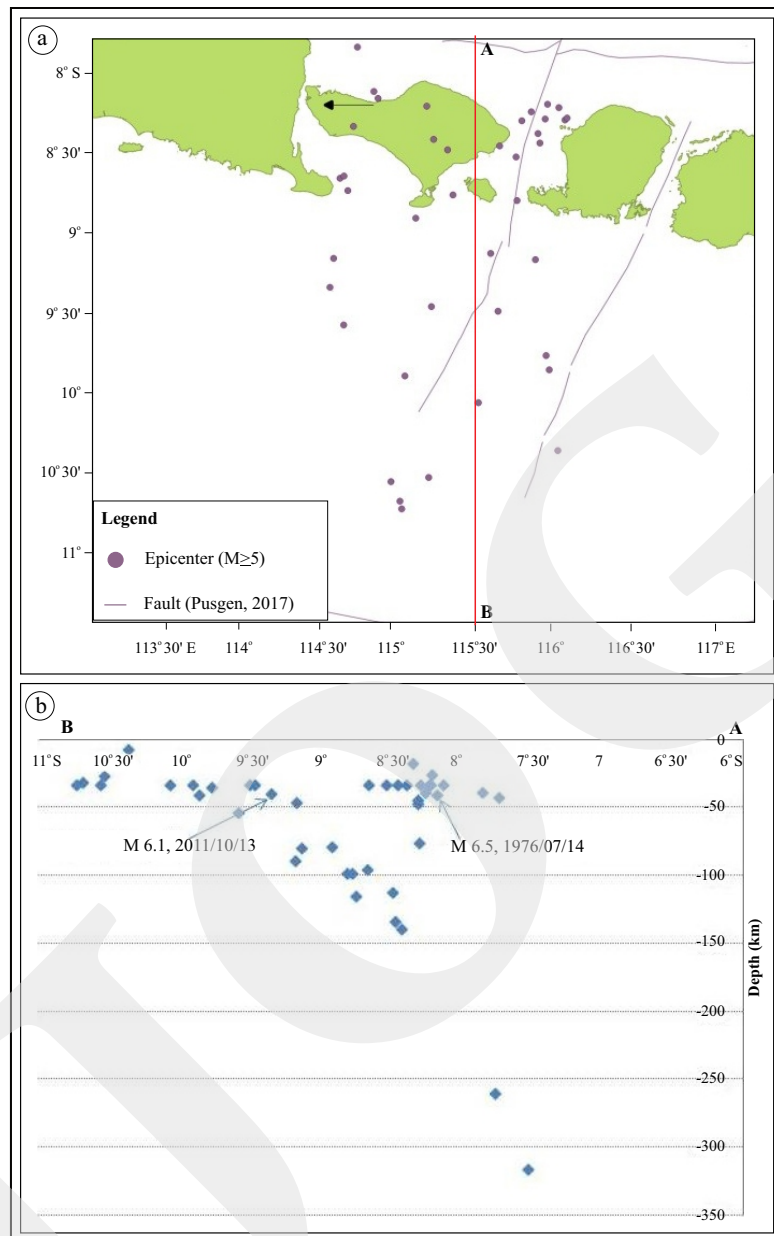


Figure 9. a) Map of earthquake distribution around Bali Island. b) Cross section of the hypocentre.

are associated with the back-arc-thrust zone that has been found deeper than 50 km (Figure 9b). Flores Back-Arc is believed to contribute to the 1976 Seririt Earthquake (Figure 9a, b) and the 1992 Flores earthquake generating tsunami. Meanwhile, twenty active faults and four potential active ones were found in Bali (Soehaemi, 2015), and the maximum magnitude of the faults are estimated to be around 6.5 Mw.

The GPS velocities are obtained from observations at fourteen GPS station networks across Bali Island. Campaign GPS sites have been

surveyed irregularly from 2013 to 2015. Using the ITRF 2008 reference system, globally the results show that the velocity of GPS sites tends to SE direction which is similar to a previous study by Bock *et al.* (2003). However, when using the movement of Sunda Block to correct the result, the direction change to NE as Koulali *et al.* (2016)'s. It seems that deformation in Bali is generated from the subduction activity in the south of Bali which can host a maximum of 7.0 Mw earthquake, followed by Flores Back-Arc Thrust at the north of Bali with 6.8 Mw. The local

fault at the eastern part of Bali (Soehaimi, 2015) can generate a 5.8 Mw earthquake. The subduction and Flores Back-Arc Thrust have the reverse fault mechanism, where the Bali Island acts as a hanging wall. The position of the island is closer to the nodal plane of the Flores-Back-Arc Thrust than to Indian-Australian Plate subduction that may explain the direction of Bali deformation to the northeast.

CONCLUSION

The horizontal velocity of Bali GPS sites varies 1.93 mm/yr to 22.53 mm/yr in NE direction, except NSDA, BTUR, and KASM to the north, and KLKG to the east. PMTR site has the smallest velocity at 1.93 mm/yr and the highest one (KLKG) at 22.53 mm/yr. While the vertical velocity ranges between -184.34 mm/yr to 33.79 mm/yr. The relative velocity may associate with the tectonic activity due to the subduction at southern Bali, West Flores Back-Arc Thrust, and East Flores Back-Arc Thrust at the northern part; and Lombok Strait Fault and a fault at eastern Bali with magnitude (Mw) 7.1, 6.6, 6.8, 5.8, and 5.2, respectively.

ACKNOWLEDGMENT

The authors are grateful to Dr. Irwan Meilano and Dr. Dina Sarsito of ITB for allowing us to use some ITB GPS sites and for the fruitful discussion. The help of dear students from Geodetic and Geomatika Department of ITB during the fieldwork is really appreciated. This work was supported the 2013-2015 fiscal year fund of the Centre for Volcanology and Geological Hazard Mitigation, Geological Agency, Indonesia.

REFERENCES

Badan Informasi Geospasial, 2015. Peta Rupa Bumi Indonesia, <http://www.bakosurtanal.go.id/peta-rupabumi/>.

- Bock, Y., Prawirodirdjo, L., Genrich, J.F., Stevens, C.W., and McCaffrey, R., 2003. Crustal Motion in Indonesia from Global Positioning System Measurements, *Journal of Geophysical Research*, 108 (B8). DOI: 10.1029/2001JB000324
- McCaffrey, R. and Nabelek, J., 1987. Earthquakes, gravity, and the origin of the Bali Basin: An example of a Nascent Continental Fold-and-Thrust Belt. *Journal of Geophysical Research*, 92 (B1) p.441-460. DOI: 10.1029/2001JB000324
- Hamilton, W.B., 1979. *Tectonic of Indonesia Region*. U.S. Govt. Printing Office, 345pp.
- Herring, T.A., King, R.W., Floyed, M.A., and McClusky, S.C., 2015. *Introduction to Gamit/Globk Release 10.6*, Massachusetts Institute of Technology, Cambridge.
- Irsyam, M., Sengara, W., Aldiarnar, F., Widiyantoro, S., Triyoso, W., Hilman, D., Kertapati, E., Meilano, I., Suhardjono, Asrurifak, M., and Ridwan, M., 2010. Development of seismic Hazard Maps of Indonesia for Revision of Seismic Hazard map in SNI 03-1726-2002, *Report of Team for Revision of Seismic Hazard Maps of Indonesia*.
- Kuncoro, H., 2013. Estimasi Parameter Rotasi Euler Blok Sunda Berdasarkan Data Pengamatan GPS Kontinyu dan Episodik di Regional Asia Tenggara, *Tesis Magister ITB*.
- Koulali, A., Susilo, S., McClusky, S., Meilano, I., Cummins, P., Tregoning, P., and Lister, G., 2016. Crustal strain partitioning and the associated earthquake hazard in the eastern Sunda-Banda Arc. *Geophysical Research Letters*, 43 (5), p.1943-1949. DOI: 10.1002/2016GL067941
- Pusat Studi Gempa Nasional (Pusgen), 2017. *Peta Sumber dan Bahaya Gempa Indonesia 2017*. Pusat Litbang Perumahan dan Pemukiman, Kemen PUPR.
- Silver, E., Donald, R., and Robert, M., 1983. Back Arc Thrusting in the Eastern Sunda Arc, *Journal of Geophysical Research*, 88 (B.09), p.7429-7448. DOI: 10.1029/JB088iB09p07429
- Soehaimi, A., 2015. *Seismotectonic and Active Fault Study of Eastern Coast Bali Island, Indonesia*. Unpublished paper.
- Sulaeman, C., 2011. Bencana Geologi di Indonesia Tahun 2011. *Buletin Vulkanologi dan Bencana*

- Geologi*, 6 (2). Badan Geologi. Bandung.
- Supartoyo, Surono, and Putranto, E.K., 2015. *Katalog Gempabumi Merusak di Indonesia Tahun 1612 - 2014*. Pusat Vulkanologi dan Mitigasi Bencana Geologi, Badan Geologi.
- Toda, S., Stein, R.S., Sevilgen, V., and Lin J., 2011. Coulomb 3.3, Graphic_Rich Deformation and Stress-Change Software for Earthquake, Tectonic, and Volcano Research and Teaching, Earthquake Science Center, Menlo Park Science Center, U.S. Geological Survey, <http://earthquake.usgs.gov/>.
- Tregoning, P., Brunner, F.K., Bock, Y., Puntodewo, S.S.O., McCaffrey, R., Genrich, J.F., Calais, E., Rais J., and Subarya, C., 1994. First Geodetic Measurement of Convergence Across the Java Trench, *Geophysical Research Letters*, 21 (19), p.2135-2138. DOI: 10.1029/94GL01856